

Directional dependence of CMB parity asymmetry

Wen Zhao*¹

*¹Department of Astronomy, University of Science
and Technology of China, Hefei, 230026, China*

*Key Laboratory for Researches in Galaxies and Cosmology,
University of Science and Technology of China, Hefei, 230026, China*

(Dated: November 14, 2018)

Abstract

Parity violation in the cosmic microwave background (CMB) radiation has been confirmed by recent Planck observation. In this paper, we extend our previous work [P. Naselsky et al. *Astrophys. J.* **749**, 31 (2012)] on the directional properties of CMB parity asymmetry by considering the Planck data of the CMB temperature anisotropy. We define six kinds of the directional statistics and find that they all indicate the odd-parity preference of CMB data. In addition, we find the preferred axes of all these statistics strongly correlate with the preferred axes of the CMB kinematic dipole, quadrupole, and octopole. The alignment between them is confirmed at more than 3σ confidence level, which implies that the CMB parity asymmetry, and the anomalies of the CMB quadrupole and octopole, may have the common physical, contaminated or systematic origin. In addition, they all should be connected with the possible contamination of the residual dipole component.

PACS numbers: 95.85.Sz, 98.70.Vc, 98.80.Cq

* Email: wzhao7@ustc.edu.cn

I. INTRODUCTION

The modern cosmological model is based on the cosmological principle: the Universe is homogeneous and isotropic on Hubble scales, which has been confirmed by various observations mainly from the isotropy of the cosmic microwave background (CMB) radiation [1, 2]. The recently released Planck data on the CMB temperature anisotropy are excellently consistent with the base Λ CDM model, especially at the high multipoles $l > 40$ [3]. However, similar to the WMAP data [4], a number of anomalies has been reported in the CMB low multipoles [5], including the low quadrupole, the alignment of the quadrupole and octopole, the missing angular power at large scale and so on. Among them, the parity asymmetry of the CMB low multipoles has also been investigated in both WMAP and Planck data [5–11], showing significant dominance of the power spectrum stored in the odd multipoles over the even ones. This anomaly of CMB may imply the physics of the early Universe [12, 13], the nontrivial topology [14, 15], some foreground residuals [10, 16] or systematic errors [17].

The connections between these anomalies have been investigated by several groups, which are helpful to reveal the physics behind them. For example, it was shown that the low quadrupole and the odd-multipole preferences were tidily connected with the lack of the two-point correlation functions in both scales $60^\circ \leq \Theta \leq 180^\circ$ [18, 19] and $1^\circ \leq \Theta \leq 30^\circ$ [20]. In Ref. [21], we have studied the directional properties of the CMB parity asymmetry in the WMAP data and found the preferred directions always coincide with the CMB kinematic dipole. Recently, the Planck team has released the CMB products SMICA (an implementation of independent component analysis of power spectra), NILC (a needlet-based version of internal linear combination), and SEVEM (template fitting using the lowest and highest frequency bands) maps, which are made via quite different techniques [22]. In this paper, applying Planck data to all these, we shall extend this work by defining six kinds of directional parity statistics. We find the preferred axes of all these statistics are quite close to each other. This indicates that the preferred axis of the CMB parity asymmetry really exists, which is independent of definitions of the statistics. Comparing with the preferred axes of the CMB quadrupole and octopole, as well as the kinematic dipole, we find the preferred axis of CMB parity asymmetry is very close to all of them. This study suggests that the CMB parity violation may have the same origin with the anomalies of CMB quadrupole and octopole, which might connect with the CMB kinematic dipole.

The outline of the paper is as follows. In Sec. 2, we introduce the basic characteristics of the CMB parity asymmetry and study the orientations of maximum parity asymmetry by defining various directional statistics. In Sec. 3, we compare this preferred axis with those of CMB kinematic dipole, quadrupole, and octopole and find the alignment between them. In Sec. 4, we summarize our investigations.

II. CMB PARITY ASYMMETRY AND THE DIRECTIONAL DEPENDENCE

The CMB temperature fluctuations on a sphere are usually decomposed as,

$$\Delta T(\theta, \phi) = \sum_{l=0}^{\infty} \sum_{m=-l}^l a_{lm} Y_{lm}(\theta, \phi), \quad (1)$$

where $Y_{lm}(\theta, \phi)$ are the spherical harmonics and a_{lm} are the corresponding coefficients. Under the assumption of the random Gaussian field, the amplitudes $|a_{lm}|$ are distributed according to Rayleigh's probability distribution function, and the phase of a_{lm} with $m \neq 0$ is supported to be evenly distributed in the range $[0, 2\pi]$. The power spectrum of CMB is defined as

$$C_l \equiv \frac{1}{2l+1} \sum_{m=-l}^l |a_{lm}|^2, \quad (2)$$

which is rotationally invariant; i.e., the power spectrum in Eq. (2) is invariant for any rotations of the reference system of the coordinate.

In the forthcoming discussion, we shall use the CMB low multipoles derived from the released Planck data, including SMICA, NILC, and SEVEM. These CMB products are made via different techniques: the SMICA map is made via spectral parameter fitting in the harmonic domain, NILC is made via a needlet variant of the internal linear combination technique, and SEVEM is constructed through template fitting using the lowest- and highest-frequency bands. These maps have the obvious differences in the Galactic plane (see Ref. [22] for details). Here, we will demonstrate that in the low multiples the biases caused by the residual contaminations in these maps are relatively small as expected. In Fig. 1, we compare the power spectra from these full-sky maps with those derived from the masked Planck Commander-Ruler (a pixel-based version of parameter and template fitting) map [22]. We find that the differences between them are indeed small, especially for the multipoles $l < 10$, which is consistent with the results in Ref. [11]. When l is larger, the biases become

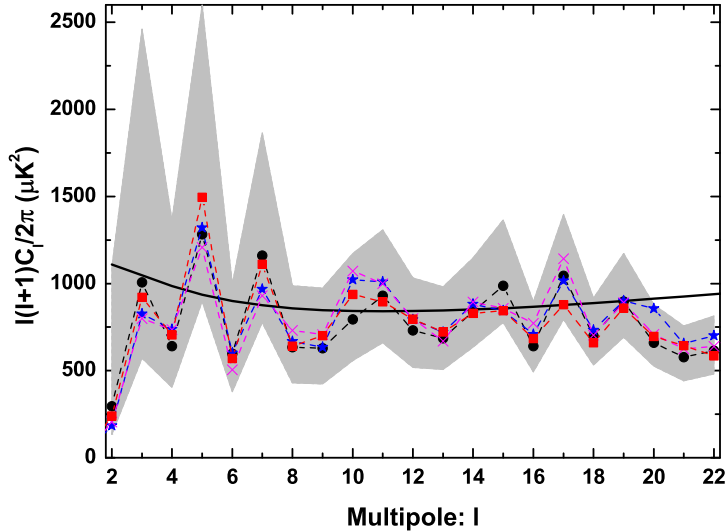


FIG. 1: The CMB power spectra at low multipoles. The black *dots* are obtained from the masked Planck C-R map, and the shadow regions are the corresponding 68% ranges on the posteriors, which are all given in the left panel of Fig. 39 in Ref. [3]. The red *squares* are the spectra derived from SMICA map, the blue *stars* are those from NILC map, and the magenta *crosses* are those from the SEVEM map.

a little more obvious, especially for the multipoles $l = 10$ and $l = 17$. However, even for these two multipoles, we find the morphologies of them derived from three maps are nearly the same (see Fig. 2), which indicates that the residual contaminations in the maps have little effect on the morphologies of the CMB low multipoles.

To study the directional properties of the CMB field, similar to Ref. [21], we can define the rotationally variant power spectrum $D(l)$ as

$$D_l \equiv \frac{1}{2l} \sum_{m=-l}^l |a_{lm}|^2 (1 - \delta_{m0}), \quad (3)$$

where $\delta_{mm'}$ is the Kronecker symbol. Note that, the definition of D_l in Eq. (3) is slightly different from that defined in Ref. [21]. For the random Gaussian, we find that $\langle D_l \rangle = C_l$; i.e., D_l is the unbiased estimator for C_l , where $\langle \dots \rangle$ denotes the average over the statistical ensemble of realizations. Compared with the spectrum in Eq. (2), in this definition, the $m = 0$ component has been excluded, so the z -axis direction has been selected as the preferred direction in this definition.

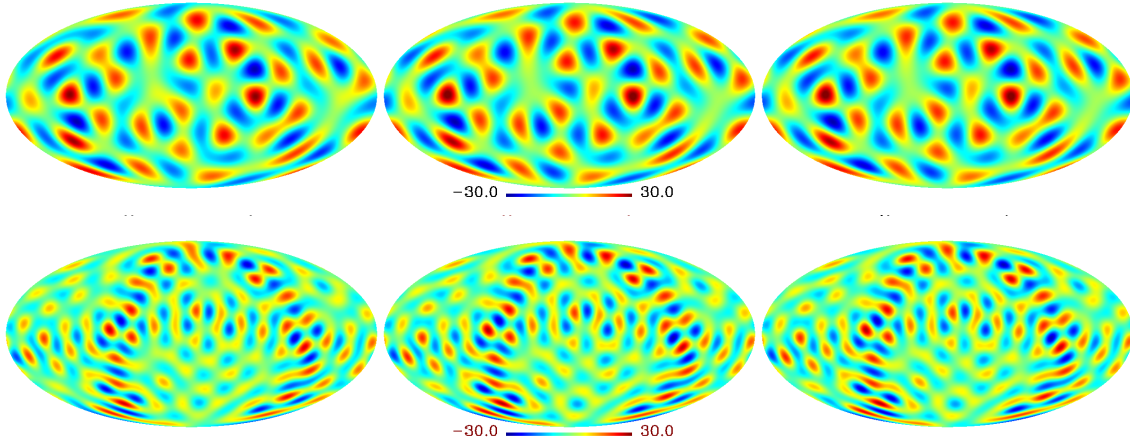


FIG. 2: The multipoles of $l = 10$ (upper) and $l = 17$ (lower). The left panels are derived from the NILC map, the middle ones are derived from the SMICA map, and the right ones are from the SEVEM map. All panels use the units μK .

Thus, we can define the power spectrum D_l in any coordinate system. Imagining the Galactic coordinate system is rotated by the Euler angle $(0, \theta, \phi)$, and the coefficients a_{lm} in this new coordinate system are calculated by

$$a_{lm}(\hat{\mathbf{q}}) = \sum_{m'=-l}^l a_{lm'} D_{mm'}^l(0, \theta, \phi), \quad (4)$$

where $\hat{\mathbf{q}} \equiv (\theta, \phi)$, a_{lm} are the coefficients defined in the Galactic coordinate system, and $D_{mm'}^l(\psi, \theta, \phi)$ is the Wigner rotation matrix. If we consider $\hat{\mathbf{q}}$ as a vector, which labels the z -axis direction in the rotated coordinate system, then (θ, ϕ) is the polar coordinate of this direction in the Galactic system. So the general power spectrum $D_l(\hat{\mathbf{q}})$ is defined as

$$D_l(\hat{\mathbf{q}}) \equiv \frac{1}{2l} \sum_{m=-l}^l |a_{lm}(\hat{\mathbf{q}})|^2 (1 - \delta_{m0}). \quad (5)$$

Now, we can define the parity statistic. As shown in Refs. [5, 7], for investigation of the parity asymmetry we can consider the statistic (see Table I)

$$g_1(l, \hat{\mathbf{q}}) = \frac{\sum_{l'=2}^l l'(l'+1) D_{l'}(\hat{\mathbf{q}}) \Gamma_{l'}^+}{\sum_{l'=2}^l l'(l'+1) D_{l'}(\hat{\mathbf{q}}) \Gamma_{l'}^-}, \quad (6)$$

where $\Gamma_l^+ = \cos^2(\frac{l\pi}{2})$ and $\Gamma_l^- = \sin^2(\frac{l\pi}{2})$. This statistic is associated with the degree of the parity asymmetry, where a value of $g_1 < 1$ indicates the odd-parity preference, and

$g_1 > 1$ indicates the even-parity preference. For any given l , the sky map of $g_1(l, \hat{\mathbf{q}})$ can be constructed by considering all the directions $\hat{\mathbf{q}}$. In practice, we pixelize the full sky in the HEALPix format with the resolution parameter $N_{\text{side}} = 64$, and set the directions $\hat{\mathbf{q}}$ to be those of the pixels.

For the temperature fluctuations of CMB map $\Delta T(\theta, \phi)$, the two-point correlation function $C(\Theta)$ is naturally defined as

$$C(\Theta, \hat{\mathbf{q}}) = \sum_{l=2}^{\infty} \frac{2l+1}{4\pi} D_l(\hat{\mathbf{q}}) P_l(\cos \Theta), \quad (7)$$

where $P_l(\cos \Theta)$ are the Legendre polynomials. Note that, in this definition the contributions of $m = 0$ components have been excluded. For the largest angular distance $\Theta = \pi$, the correlation function is

$$C(\Theta = \pi, \hat{\mathbf{q}}) = \sum_{l=2}^{\infty} \frac{2l+1}{4\pi} D_l(\hat{\mathbf{q}}) (\Gamma_l^+ - \Gamma_l^-). \quad (8)$$

So the natural way to estimate the relative contribution of even and odd multipoles to the correlation function is to define the statistic [21] (see Table I),

$$g_2(l, \hat{\mathbf{q}}) = \frac{\sum_{l'=2}^l (2l'+1) D_{l'}(\hat{\mathbf{q}}) \Gamma_{l'}^+}{\sum_{l'=2}^l (2l'+1) D_{l'}(\hat{\mathbf{q}}) \Gamma_{l'}^-}, \quad (9)$$

which follows that $C(\Theta = \pi) \propto (g_2(l, \hat{\mathbf{q}}) - 1)$. $g_2 > 1$ corresponds to the positive correlation of the opposite directions, and $g_2 < 1$ indicates the anticorrelation of them. Note that the statistic g_2 is different from g_1 , due to the different factors before D_l in their definitions. Therefore, the relative weights of low multipoles are much higher in g_2 than those in g_1 .

For further investigation, in this paper we also consider the third statistic to quantify the parity asymmetry, which was first introduced in Ref. [11] (see Table I),

$$g_3(l, \hat{\mathbf{q}}) = \frac{2}{l-1} \sum_{l'=3}^l \frac{(l'-1)l' D_{l'-1}(\hat{\mathbf{q}})}{l'(l'+1) D_{l'}(\hat{\mathbf{q}})}, \quad (10)$$

where the maximum, l , is any odd multipole $l \geq 3$ and the summation is over all odd multipoles up to l . This statistic is the measure of the mean deviation of the ratio of power in an even multipole to its succeeding odd-multipole form one.

In previous works [5, 7, 8, 11], by using the power spectrum C_l , the authors found that CMB parity asymmetry is quite significant at the low multipoles, and this tendency extends to the multipole range $l < 22$. Since the definition of the estimator D_l is similar to that

TABLE I: The definitions of six directional statistics considered in the text.

Number of statistic	Definition
1 st	$g_1(l, \hat{\mathbf{q}})$ with $D_l(\hat{\mathbf{q}})$
2 nd	$g_2(l, \hat{\mathbf{q}})$ with $D_l(\hat{\mathbf{q}})$
3 rd	$g_3(l, \hat{\mathbf{q}})$ with $D_l(\hat{\mathbf{q}})$
4 th	$g_1(l, \hat{\mathbf{q}})$ with $\tilde{D}_l(\hat{\mathbf{q}})$
5 th	$g_2(l, \hat{\mathbf{q}})$ with $\tilde{D}_l(\hat{\mathbf{q}})$
6 th	$g_3(l, \hat{\mathbf{q}})$ with $\tilde{D}_l(\hat{\mathbf{q}})$

of C_l , one expects the parity asymmetry of the statistics g_1 , g_2 , g_3 to also extend to this multipole range. We apply these three statistics for all the odd multipoles $3 \leq l \leq 21$ to the released Planck SMICA, NILC and SEVEM data. The results for SMICA data are presented in Fig. 3. For all the odd maximum multipoles l and directions $\hat{\mathbf{q}}$, we have $g_i < 1$ for $i = 1, 2, 3$. These are also correct for Planck NILC and SEVEM data. So consistent with previous works [5, 7, 8, 11, 21], we find that the real CMB data have the odd-parity preference, which is independent of the choice of the parity statistics.

To cross-check the results, we consider another rotationally variant estimator, proposed in Refs. [5, 21, 23, 24],

$$\tilde{D}_l \equiv \frac{1}{2l+1} \sum_{m=-l}^l m^2 |a_{lm}|^2. \quad (11)$$

As well discussed, this statistic has also selected the z -axis direction as the preferred direction. However, we should mention that this estimator, \tilde{D}_l , is definitely different from D_l defined in Eq. (3). First, for each multipole l , the components a_{lm} with $m \neq 0$ have the exact same weights in the definition of D_l , which shows that this statistic only favors the component $m = 0$. But from Eq. (11), we know that \tilde{D}_l favors the high ms and so it works well in searches for planarity (i.e., $m = \pm l$) [23, 24]. Secondly, comparing the different multipoles, we find that due to the factor m^2 in the definition, the value of \tilde{D}_l increases dramatically with the increasing of the multipole number l , which is also different from that of D_l .

Because of the rotational variance of this quantity, we can define the general power

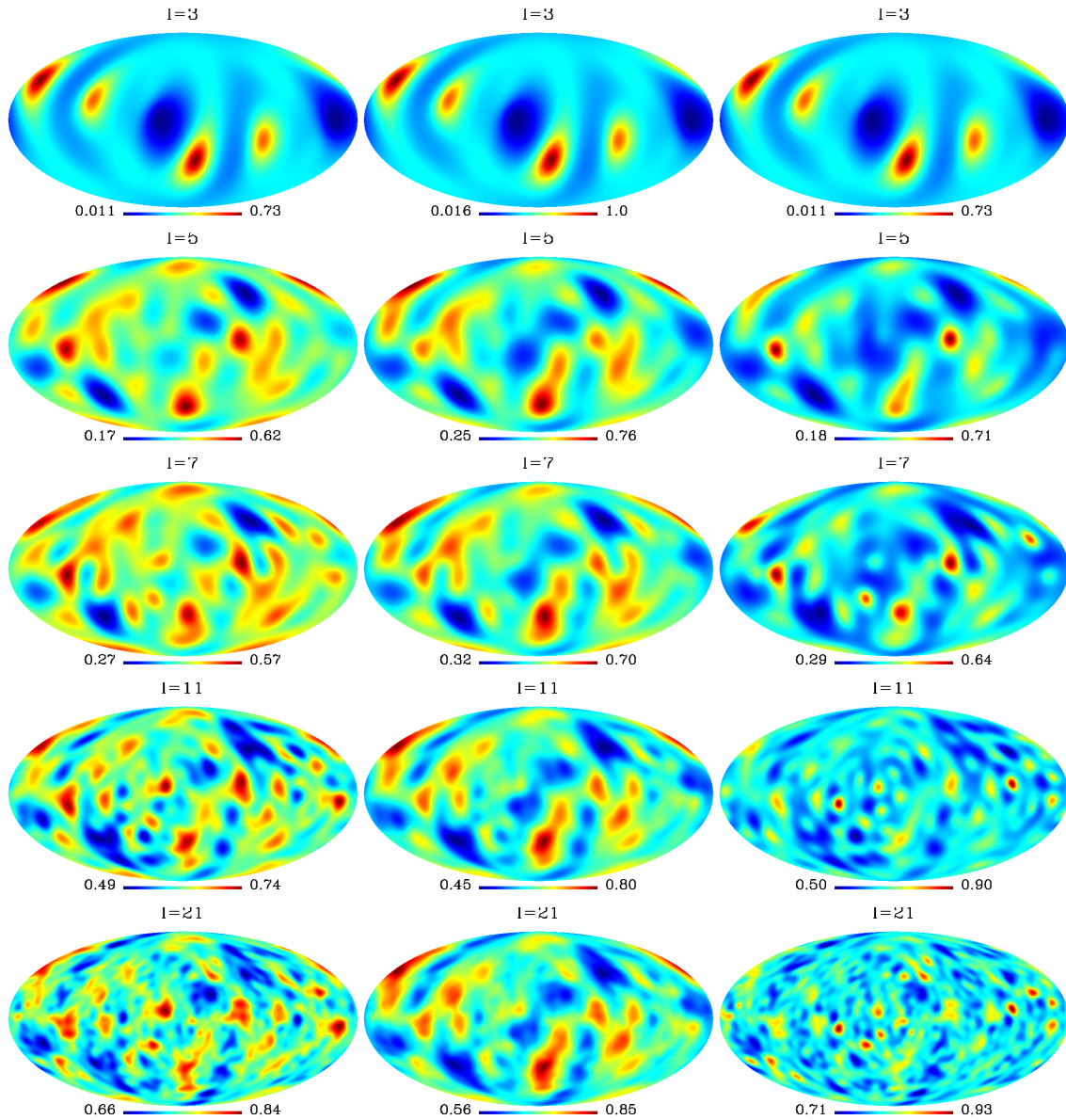


FIG. 3: Three directional statistics $g_1(l, \hat{\mathbf{q}})$ (left), $g_2(l, \hat{\mathbf{q}})$ (middle), and $g_3(l, \hat{\mathbf{q}})$ (right) as functions of $\hat{\mathbf{q}} \equiv (\theta, \phi)$. Note that, these results are based on the Planck SMICA data.

spectrum as

$$\tilde{D}_l(\hat{\mathbf{q}}) \equiv \frac{1}{2l+1} \sum_{m=-l}^l m^2 |a_{lm}(\hat{\mathbf{q}})|^2, \quad (12)$$

where $a_{lm}(\hat{\mathbf{q}})$ is defined in Eq. (4). Thus, the other three directional statistics can be defined

as follows (see also Table I):

$$g_4(l, \hat{\mathbf{q}}) = g_1(l, \hat{\mathbf{q}})|_{D_l \rightarrow \tilde{D}_l}, \quad (13)$$

$$g_5(l, \hat{\mathbf{q}}) = g_2(l, \hat{\mathbf{q}})|_{D_l \rightarrow \tilde{D}_l}, \quad (14)$$

$$g_6(l, \hat{\mathbf{q}}) = g_3(l, \hat{\mathbf{q}})|_{D_l \rightarrow \tilde{D}_l}. \quad (15)$$

As we have emphasized, the estimator \tilde{D}_l is quite different from D_l due to the factor m^2 in the definition. In the statistics g_4 , g_5 , or g_6 , the contributions of the higher multipoles, $l \sim l_{\max}$, become completely dominant. For this reason, we only apply these statistics to the multipole range in which the CMB parity asymmetry is most obvious. Although, in Refs. [5, 21], the authors found the CMB parity asymmetry can extend to multipole ranges up to $l \sim 22$, the main contribution comes from the lowest multipoles, i.e., $l < 10$, which can be clearly seen in the following facts. From Fig. 1, we find that the regular oscillation of the power spectra (i.e., the values of even multipoles are significantly smaller, while those of odd multipoles are significantly larger, which is the performance of the CMB parity asymmetry) is obvious only in the multipole range $l < 10$. Consistently, from Fig. 1 in Refs. [21], we also find that the CMB parity asymmetry becomes negligible if the low multipoles $l < 10$ are excluded. So, the same as in Ref. [21], in this paper we only consider the parity statistics g_4 , g_5 , and g_6 for the multipoles $l < 10$.

We apply these three statistics to the Planck SMICA, NILC, and SEVEM data and find similar results. In Fig.4, we present the results of SMICA data, which show that $g_i(l, \hat{\mathbf{q}}) < 1$ ($i = 4, 5, 6$) are held for any direction $\hat{\mathbf{q}}$. So we conclude that the odd-parity preference exists even if the estimator \tilde{D}_l is considered.

III. CORRELATION WITH THE PREFERRED AXES OF OTHER CMB OBSERVATIONS

Now, let us investigate how the parity statistics depend on the direction $\hat{\mathbf{q}}$. From Fig.3, we find that all the statistics $g_i(l, \hat{\mathbf{q}})$ of $i = 1, 2, 3$ have a quite similar morphology for $l > 3$, although the weights of the multipoles in their definitions are different. The similar results have also been found for the statistics $g_i(l, \hat{\mathbf{q}})$ of $i = 4, 5, 6$ in Fig.4. In particular, from these two figures, we find that the panels of $l > 3$ have the similar preferred directions $\hat{\mathbf{q}}$, where the corresponding parity statistic is minimized. These have also been clearly shown

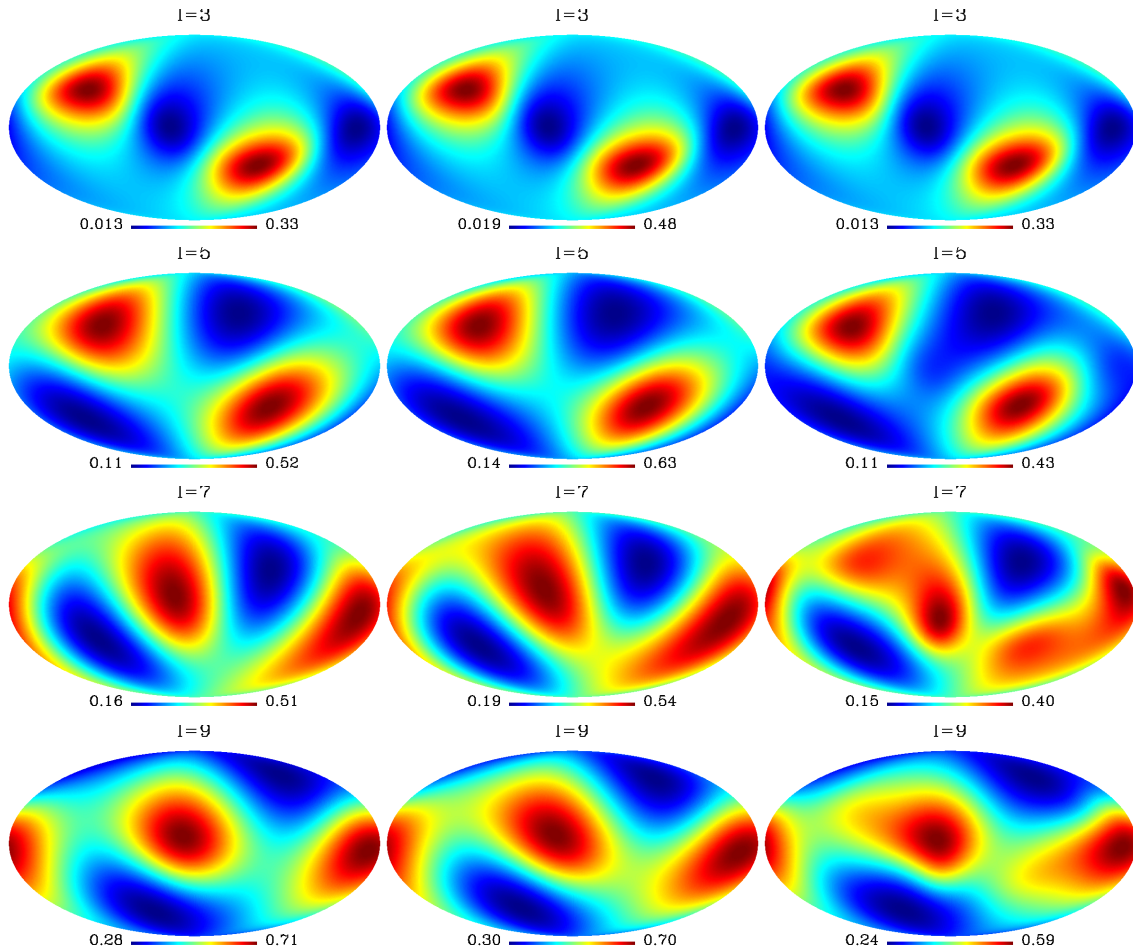


FIG. 4: Three directional statistics $g_4(l, \hat{\mathbf{q}})$ (left), $g_5(l, \hat{\mathbf{q}})$ (middle), and $g_6(l, \hat{\mathbf{q}})$ (right) as functions of $\hat{\mathbf{q}} \equiv (\theta, \phi)$. Note that, these results are based on the Planck SMICA data.

in Tables II and III. Meanwhile, the same results are also confirmed in NILC and SEVEM maps [39].

In Fig.5, we compare the preferred directions $\hat{\mathbf{q}}$ of parity asymmetry with the CMB kinematic dipole and find they are very close to each other. Especially, all these directions are close to the ecliptic plane. To quantify it, we define the quantity α , which is the angle between $\hat{\mathbf{q}}$ and the CMB kinematic dipole direction at $(\theta = 42^\circ, \phi = 264^\circ)$ [25]. We list the values of $|\cos \alpha|$ in Tables II-V and find that all of them are very close to 1. Note that, throughout this paper we do not differentiate the direction $\hat{\mathbf{q}}$ and the opposite one $-\hat{\mathbf{q}}$.

In both WMAP and Planck data, the alignment between the orientation of the CMB quadrupole and octopole has been reported. In the Planck SMICA data, the preferred

direction of the quadrupole is at $(\theta = 13.4^\circ, \phi = 238.5^\circ)$, and that of octopole is $(\theta = 25.7^\circ, \phi = 239.0^\circ)$ [5]. The angle between them is 12.3° , and the significance of alignment is 96.8%. Such a level may not necessarily correspond to a statistical significance. However, when combined with the axes directions of other cosmological observations, such as the anisotropy of cosmic acceleration, the bulk velocity flow axis, and the quasar optical polarization alignment axis, the statistical evidence of the relative coincidence could increase dramatically (see, for instance, Ref. [26]).

In this paper, we shall investigate whether or not the alignment of quadrupole and octopole connects with the parity asymmetry. Following Ref. [26], it is straightforward to evaluate the mean value of the inner product between all the pairs of unit vectors corresponding to the following four directions: the preferred directions of quadrupole, octopole, parity asymmetry and the direction of the CMB kinematic dipole. So, we define the quantity,

$$\langle |\cos \theta_{ij}| \rangle = \sum_{i,j=1, j \neq i}^N \frac{|\hat{r}_i \cdot \hat{r}_j|}{N(N-1)}, \quad (16)$$

where N is the number of the directions, which will be investigated. First, we shall study the case in the absence of the parity asymmetry. The alignment between these three axes was also reported in WMAP data [18]. In this case, we have $N = 3$ and $\langle |\cos \theta_{ij}| \rangle = 0.9242$ for the real data. To evaluate the significance of the alignment, we pixelize the two-dimensional sphere in the HEALPix format with the resolution parameter $N_{\text{side}} = 256$, which corresponds to the total pixel number $N_{\text{pix}} = 12 \times N_{\text{side}}^2$. Then, we randomly generate 10^5 realizations. For each realization, the three directions are randomly and independently picked on the sky using a uniform distribution between 0 and $N_{\text{pix}} - 1$, and the corresponding value $\langle |\cos \theta_{ij}| \rangle$ is calculated directly. Considering all the random samples, we obtain that $\langle |\cos \theta_{ij}| \rangle = 0.500 \pm 0.167$. To quantify the significant level of the deviation from the random distribution, we define the Δ_c/σ_c , where Δ_c is the difference between the observed value of $\langle |\cos \theta_{ij}| \rangle$ and the mean value of the simulations, and σ_c is the corresponding standard deviation of the simulations. Considering the observed result $\langle |\cos \theta_{ij}| \rangle = 0.9242$, and the simulated value $\sigma_c = 0.167$, we obtain that $\Delta_c/\sigma_c = 2.54$, which indicates that the alignment of these three directions is around 2.5σ confidence level.

Now, let us take into account the preferred direction of the CMB parity asymmetry. For the 10^5 random realizations of four random points on the sphere, by a similar analysis, we

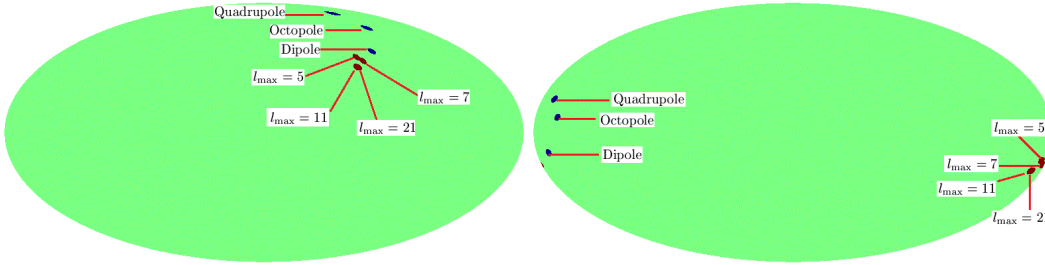


FIG. 5: The preferred directions of the SMICA-based statistics $g_1(l, \hat{\mathbf{q}})$ in the Galactic coordinate system (left) and in the ecliptic coordinate system (right). In both panels, we have compared them with the CMB kinematic dipole direction and the preferred directions of the CMB quadrupole and octopole.

get

$$\langle |\cos \theta_{ij}| \rangle = 0.500 \pm 0.118. \quad (17)$$

As anticipated, compared with the case of $N = 3$, the mean value stays the same, while the standard deviation σ_c significantly decreases. Now, we calculate the real value of the quantity $\langle |\cos \theta_{ij}| \rangle$. For the preferred direction of parity asymmetry, we consider the results of all the six statistics $g_i(l, \hat{\mathbf{q}})$ defined in this paper, and list the corresponding values in Tables II-V. For every case with $l > 3$, we find that $\langle |\cos \theta_{ij}| \rangle$ is close to 0.9, and the corresponding significance of the alignment between these directions increases to $\Delta_c/\sigma_c \gtrsim 3$.

We therefore conclude that the preferred direction of the CMB parity asymmetry is not only very close to the CMB kinematic dipole, but also close to the preferred axes of the CMB quadrupole and octopole, which is nearly independent of the choice of the parity statistic. Their coexistence in a relatively small angular region is a very unlikely event, which implies that these anomalies have a common origin: an undiscovered physical effect or a common basic systematic error that has so far escaped attention.

IV. CONCLUSIONS

Parity violation is one of the anomalies of the CMB temperature anisotropy map in the large scales, which may indicate the nontrivial topology of the Universe, the physics of the

TABLE II: The preferred direction $\hat{\mathbf{q}} = (\theta, \phi)$, where the parity parameter $g_i(l, \hat{\mathbf{q}})$ based on Planck SMICA data is minimized, is compared with the other CMB preferred axes. In each box, the upper one is the result for the statistic with $i = 1$, the middle one is that for $i = 2$, and the lower one is that for $i = 3$. In this table, α is the angle between $\hat{\mathbf{q}}$ and the CMB kinematic dipole, $\langle |\cos \theta_{ij}| \rangle$ is the quantity defined in Eq. (16), and the Δ_c/σ_c value denotes the number of σ_c the observed $\langle |\cos \theta_{ij}| \rangle$ deviate from the simulations.

	$\theta[^\circ]$	$\phi[^\circ]$	$ \cos \alpha $	$\langle \cos \theta_{ij} \rangle$	Δ_c/σ_c
$l_{\max} = 3$	90.00	23.20	0.3265	0.6066	0.90
	90.00	23.20	0.3265	0.6066	0.90
	90.00	23.20	0.3265	0.6066	0.90
$l_{\max} = 5$	45.80	281.07	0.9767	0.9015	3.40
	45.80	281.07	0.9767	0.9015	3.40
	45.80	281.07	0.9767	0.9015	3.40
$l_{\max} = 7$	48.19	277.73	0.9799	0.8979	3.37
	47.39	279.29	0.9782	0.8987	3.38
	52.83	267.89	0.9710	0.8915	3.32
$l_{\max} = 11$	52.08	284.06	0.9525	0.8744	3.17
	49.77	280.54	0.9697	0.8886	3.29
	53.58	226.41	0.8679	0.8793	3.21
$l_{\max} = 21$	52.08	285.47	0.9479	0.8721	3.15
	50.55	284.06	0.9575	0.8804	3.22
	21.32	131.90	0.5292	0.8295	2.79

early inflation, the foreground residuals, or some unsolved systematic errors. In this paper, we have extended our previous work on the directional properties of the CMB parity violation and applied to the newly released Planck data. We have defined two kinds of rotationally variant power spectra $D_l(\hat{\mathbf{q}})$ and $\tilde{D}_l(\hat{\mathbf{q}})$, where the special direction had been selected in the definitions. Based on these estimators, we considered six different parity statistics, and demonstrated the direction preferences of the CMB parity asymmetry in the low multipoles.

TABLE III: The preferred direction $\hat{\mathbf{q}} = (\theta, \phi)$, where the parity parameter $g_i(l, \hat{\mathbf{q}})$ based on Planck SMICA data is minimized, is compared with the other CMB preferred axes. In each box, the upper one is the result for the statistic with $i = 4$, the middle one is that for $i = 5$, and the lower one is that for $i = 6$. In this table, α is the angle between $\hat{\mathbf{q}}$ and the CMB kinematic dipole, $\langle |\cos \theta_{ij}| \rangle$ is the quantity defined in Eq. (16), and the Δ_c/σ_c value denotes the number of σ_c the observed $\langle |\cos \theta_{ij}| \rangle$ deviate from the simulations.

	$\theta[^\circ]$	$\phi[^\circ]$	$ \cos \alpha $	$\langle \cos \theta_{ij} \rangle$	Δ_c/σ_c
$l_{\max} = 3$	88.81	23.20	0.3109	0.5975	0.83
	88.81	23.20	0.3109	0.5975	0.83
	88.81	23.20	0.3109	0.5975	0.83
$l_{\max} = 5$	47.39	307.86	0.8582	0.8458	2.93
	47.39	310.71	0.8408	0.8390	2.87
	46.59	309.92	0.8488	0.8442	2.92
$l_{\max} = 7$	62.72	280.55	0.9107	0.8306	2.80
	56.49	281.25	0.9431	0.8599	3.05
	55.77	281.95	0.9443	0.8621	3.07
$l_{\max} = 9$	32.60	236.25	0.9451	0.9424	3.75
	36.43	248.88	0.9815	0.9418	3.74
	34.89	246.06	0.9737	0.9435	3.76

Similar to the statistics based on the rotationally invariant estimator C_l , we found all these statistics show the odd-parity preference of the CMB data. At the same time, we found that the preferred directions $\hat{\mathbf{q}}$ of all the statistics, where the statistics are minimized, are very close to each other as long as $l > 3$. In particular, these preferred directions are close to both the direction of the CMB kinematic dipole and the preferred directions of the CMB quadrupole and octopole. The confident level of the deviation from the random distribution between them is $\Delta_c/\sigma_c \gtrsim 3$, which implies that the parity violation and the anomalies of the CMB quadrupole and octopole might have the common dipole-related origin. This origin might be in physics, in contamination or in systematics. In any case, the future polarization data, TE , EE , and BB would be helpful to resolve the puzzles and the coincidence between

TABLE IV: The values of $|\cos \alpha|$ and Δ_c/σ_c for the statistics $g_i(l, \hat{\mathbf{q}})$ based on Planck NILC and SEVEM data. Similar to Table II, in each box, the upper one is the result for the statistic with $i = 1$, the middle one is that for $i = 2$, and the lower one is that for $i = 3$.

	$ \cos \alpha $ for NILC	Δ_c/σ_c for NILC	$ \cos \alpha $ for SEVEM	Δ_c/σ_c for SEVEM
$l_{\max} = 3$	0.3259	0.88	0.2656	0.66
	0.3259	0.88	0.2656	0.66
	0.3259	0.88	0.2656	0.66
$l_{\max} = 5$	0.9758	3.38	0.9802	3.42
	0.9748	3.36	0.9802	3.42
	0.9748	3.36	0.9802	3.42
$l_{\max} = 7$	0.9822	3.37	0.9840	3.41
	0.9769	3.36	0.9812	3.39
	0.9812	3.33	0.9861	3.37
$l_{\max} = 11$	0.8600	3.18	0.8600	3.18
	0.9697	3.29	0.9766	3.34
	0.8520	3.15	0.8600	3.18
$l_{\max} = 21$	0.8932	3.25	0.9529	3.19
	0.9575	3.22	0.9575	3.22
	0.8522	3.13	0.5295	2.79

them.

In the end, it is interesting to mention that several preferred axes have also been reported in other cosmological observations: velocity flows [27], quasar alignment [28], anisotropies of the cosmic acceleration [29, 30], the dipole in the handedness of spiral galaxies [31], and the dipole effect of the fine structure constant [32] (see Ref. [33] as a review). Although there is still some debate [34–36], it has been claimed that these preferred directions are also aligned with the CMB kinematic dipole and the preferred direction of CMB quadrupole and octopole [33]. If all the directional preferences would be confirmed in the future, it would imply that the underlying physical or systematic reasons of all the cosmological anomalies

TABLE V: The values of $|\cos \alpha|$ and Δ_c/σ_c for the statistics $g_i(l, \hat{\mathbf{q}})$ based on Planck NILC and SEVEM data. Similar to Table III, in each box the upper one is the result for the statistic with $i = 4$, the middle one is that for $i = 5$ and the lower one that is for $i = 6$.

	$ \cos \alpha $ for NILC	Δ_c/σ_c for NILC	$ \cos \alpha $ for SEVEM	Δ_c/σ_c for SEVEM
$l_{\max} = 3$	0.3094	0.78	0.2650	0.64
	0.3094	0.78	0.2650	0.64
	0.3094	0.78	0.2650	0.64
$l_{\max} = 5$	0.8705	3.06	0.9040	3.16
	0.8705	3.06	0.8963	3.13
	0.8617	3.03	0.8963	3.13
$l_{\max} = 7$	0.9838	3.37	0.9585	3.14
	0.9852	3.43	0.9710	3.26
	0.9782	3.38	0.9693	3.28
$l_{\max} = 9$	0.9097	3.73	0.9351	3.74
	0.9450	3.77	0.9713	3.77
	0.9290	3.75	0.9529	3.77

should be connected.

Acknowledgements: We acknowledge the use of the Planck Legacy Archive (PLA). Our data analysis made the use of HELAPix [37] and GLESP [38]. This work is supported by Project 973 under Grant No.2012CB821804; NSFC under Grants No.11173021, No.11075141, No.11322324; and a project of KIP of CAS.

-
- [1] C.L. Bennett et al., *Astrophys. J. Suppl. Ser.* **148**, 1 (2003).
 - [2] Planck Collaboration, arXiv:1303.5062.
 - [3] Planck Collaboration, arXiv:1303.5076.
 - [4] C.L. Bennett et al., *Astrophys. J. Suppl. Ser.* **192**, 17 (2011).

- [5] Planck Collaboration, arXiv: 1303.5083.
- [6] K. Land and J. Magueijo, *Mon. Not. Roy. Astron. Soc.* **378**, 153 (2007).
- [7] J. Kim and P. Naselsky, *Astrophys. J.* **714**, L265 (2010).
- [8] J. Kim and P. Naselsky, *Phys. Rev. D***82**, 063002 (2010).
- [9] A. Gruppuso, F. Finelli, P. Natoli, F. Paci, P. Cabella, A. De Rosa and N. Mandolesi, *Mon. Not. Roy. Astron. Soc.* **411**, 1445 (2011).
- [10] M. Hansen, J. Kim, A.M. Frejsel, S. Ramazanov, P. Naselsky, W. Zhao and C. Burigana, *JCAP* **10**, 059 (2012).
- [11] P.K. Aluri and P. Jain, *Mon. Not. Roy. Astron. Soc.* , **419** 3378 (2012).
- [12] H. Liu, A.M. Frejsel and P. Naselsky, *JCAP* **07**, 032 (2013).
- [13] X. Chen and Y. Wang, arXiv:1305.4794.
- [14] Planck Collaboration, arXiv:1303.5086.
- [15] Z. Chang and S. Wang, *Eur. Phys. J. C***73**, 2516 (2013).
- [16] M. Maris, C. Burigana, A. Gruppuso, F. Finelli and J.M. Diego, *Mon. Not. Roy. Astron. Soc.* **415**, 2546 (2011).
- [17] H. Liu and T. Li, *Astrophys. J.* **732**, 125 (2011).
- [18] D.J. Schwarz, G.D. Starkman, D. Huterer and C. Copi, *Phys. Rev. Lett.* **93**, 221301 (2004).
- [19] C. Copi, D. Huterer, D.J. Schwarz and G.D. Starkman, *Adv. Astron.* **2010**, 1 (2010).
- [20] J. Kim and P. Naselsky, *Astrophys. J.* **739**, 79 (2011).
- [21] P. Naselsky, W. Zhao, J. Kim and S. Chen, *Astrophys. J.* **749**, 31 (2012).
- [22] Planck Collaboration, arXiv: 1303.5072.
- [23] A. de Oliveira-Costa, M. Tegmark, M. Zaldarriaga and A. Hamilton, *Phys. Rev. D***69**, 063516 (2004).
- [24] K. Land and J. Magueijo, *Phys. Rev. Lett.* **95**, 071301 (2005).
- [25] Planck Collaboration, arXiv: 1303.5087.
- [26] I. Antoniou and L. Perivolaropoulos, *JCAP* **12**, 012 (2010).
- [27] H.A. Feldman, R. Watkins and M.J. Hudson, *Mon. Not. Roy. Astron. Soc.* **407**, 2328 (2010).
- [28] D. Hutsemekers, R. Cabanac, H. Lamy and D. Sluse, *Astron. Astrophys.* **441**, 915 (2005).
- [29] I. Antoniou and L. Perivolaropoulo, *JCAP* **12**, 012 (2010).
- [30] R.G. Cai and Z.L. Tuo, *JCAP* **02**, 004 (2012).
- [31] M. J. Longo, *Phys. Lett. B***699**, 224 (2011).

- [32] A. Mariano and L. Perivolaropoulos, *Phys. Rev. D* **86**, 083517 (2012).
- [33] L. Perivolaropoulos, arXiv:1104.0539.
- [34] B. Kalus, D.J. Schwarz, M. Seikel and A. Wiegand, *Astron. Astrophys.* **553**, A56 (2013).
- [35] R.G. Cai, Y.Z. Ma, B. Tang and Z.L. Tuo, *Phys. Rev. D* **87**, 123522 (2013).
- [36] W. Zhao, P.X. Wu and Y. Zhang, *Int. J. Mod. Phys. D* **22**, 1350060 (2013).
- [37] K.M. Gorski, E. Hivon, A.J. Banday, B.D. Wandelt, F.K. Hansen, M. Reinecke and M. Bartelman, *Astrophys. J.* **622**, 759 (2005).
- [38] A.G. Doroshkevich, P.D. Naselsky, O.V. Verkhodanov, D.I. Novikov, V.I. Turchaninov, I.D. Novikov, P.R. Christensen and L.Y. Chiang, *Int. J. Mod. Phys. D* **14**, 275 (2005).
- [39] Similar to Ref. [21], in both figures, we find that the morphologies of $l = 3$ maps are different from others, which may connect with the detailed origin of the anomalous CMB quadrupole and octopole and needs further investigation.